Side-Opened Suspended Core Fiber-Based Surface Plasmon Resonance Sensor

Guanjun Wang, Chao Wang, Shen Liu, Jing Zhao, Changrui Liao, Xizhen Xu, Haijian Liang, Guolu Yin, and Yiping Wang

***Abstract*—An integrated surface plasmon resonance (SPR) based on an Au-film-coated, side-opened suspended core fiber is proposed and simulated to develop a highly sensitive, real-time refractive index sensor. The inner surface of the side-opened hole is supposed to be uniformly deposited with a thin Au film for realizing the SPR operation. Such a sensor not only ensures a fast response time, but also brings up a designing flexibility for SPR biosensing applications. Two potential sensing mechanisms, i.e., monitoring the transmission loss spectrum peak shift and measuring the transmission power change at a fixed wavelength are utilized and analyzed to achieve a better sensitivity. Moreover, our calculation results show that this novel sensor could cover a wide index detection range with an optimized resolution of up to 2.3e−5 refractive index unit.**

***Index Terms*—Surface plasmon resonance sensor, suspended core fiber, side-opened.**

I. Introduction

THE demand of fast responsive, high sensitive, integrated and label-free bio-chemical sensing is of vast importance in many areas, such as cancer biomarker detection [1]. Many types of integrated biosensors and their sensing characteristics have been proposed and analyzed during the past years [1]–[13], especially fiber sensors. Fiber-based surface Plasmon resonance (SPR) sensors are widely used for bio-chemical sensing due to its characteristic of high sensitivity to refractive index change in the surface plasmon state [8]. While miniaturization and integration of the SPR systems could also be realized by utilizing the optical fiber configuration [9]–[16]. Other advantages of the optical fiber-based SPR sensors include the possibility of label-free biochemical detection, simplified design, and the feasibility of the remote or distributive detection. Besides, the surface Plasmon resonance enhanced surface intensity can also contribute to the Raman scattering and the fluorescence excitation applications [17], [18].

For the optical fiber-based SPR sensors, the angle of the incident light is generally fixed. Broadband optical source or single wavelength laser are always utilized for the spectrum demodulation or intensity demodulation setups. When the resonance coupling occurs between the fundamental mode and the surface Plasmon mode, a sharp peak could be appeared in the transmission loss spectrum and used for calculating the refractive index of the target. SPR sensor based on many kinds of fibers, such as single mode fiber (SMF) [9], multimode fiber (MMF) [7] and conventional photonic crystal fiber (PCF) [11]–[16] structures, have been demonstrated. But, it seems that the abovementioned structures exhibit some drawbacks. For examples, SPR sensors based on SMF and MMF always suffer from a less sensitivity and a low surface intensity due to the insufficient sharp transmission loss peak [9], [10]. PCF-based SPR sensors require a long response time due to the slow fluid filling speed. While tapered fiber based SPR sensor is fragile in handling [19].

To decrease the response time, side hole [20] and side polished [21], [22] designs were applied in building fiber SPR sensor. It seems that such designs could enhance both the response time and the sensitivity properties of sensors. However, there is still a large space for improvement. In this article, a novel high sensitive, fast responsive fiber SPR sensor design based on the side-opened suspended core fiber is proposed and analyzed. The struts' surface facing the opening hole is supposed to be uniformly deposited with an Au-film for realizing the surface plasmon resonance. Thus the low efficient, time-consuming metal film deposition process from fluids passing along the length of the holes of conventional side-closed suspended core fiber is avoided. Since the thickness and length of Au thin film could be controlled conveniently via the side opening in fiber, the single hole-coated fiber configuration provide a designing flexibility for the SPR sensing applications. In addition, this side opening configuration could ensure a fast response characteristic of less than 9s, which was provided in our previous reports [23], [24]. The fast response characteristic could be applied in real-time

Manuscript received June 13, 2014; revised November 30, 2014; accepted December 2, 2014. Date of publication December 24, 2014; date of current version May 20, 2015. This work was supported in part by the National Natural Science Foundation of China under Grant 11174064, Grant 61377090, Grant 61405127, Grant 61425007, and Grant 61308027, in part by the Science and Technology Innovation Commission of Shenzhen/Nanshan under Grant JCYJ20130329140017262, Grant KQCX20120815161444632, Grant ZDSYS20140430164957664, and Grant KC2014ZDZJ0008A, in part by the Science Foundation of North University of China, in part by the China Post-Doctoral Science Foundation under Grant 2014M562202, in part by the Shanxi Province Science Foundation for Youths under Grant 2014021023-1, and in part by the Pearl River Scholar Fellowships. The associate editor coordinating the review of this paper and approving it for publication was Dr. Anna G. Mignani. *(Corresponding author: Yiping Wang.)*

G. Wang is with the Key Laboratory of Optoelectronic Devices and Systems of Ministry of Education and Guangdong Province, College of Optoelectronic Engineering, Shenzhen University, Shenzhen 518060, China, and also with the Shanxi Provincial Research Center for Opto-electronic Information and Instrument Engineering Technology, North University of China, Taiyuan 030051, China (e-mail: wangguanjun@163.com).

C. Wang, S. Liu, J. Zhao, C. Liao, X. Xu, H. Liang, G. Yin, and Y. Wang are with the Key Laboratory of Optoelectronic Devices and Systems of Ministry of Education and Guangdong Province, College of Optoelectronic Engineering, Shenzhen University, Shenzhen 518060, China (e-mail 3752601@qq.com; liushen.szu@gmail.com; zhaojing090824@163.com; cliao@szu.edu.cn; 406434774@qq.com; 1518472969@qq.com; guoluyin@gmail.com; ypwang@szu.edu.cn).

Color versions of one or more of the figures in this paper are available online at http://ieeexplore.ieee.org.

Digital Object Identifier 10.1109/JSEN.2014.2382612

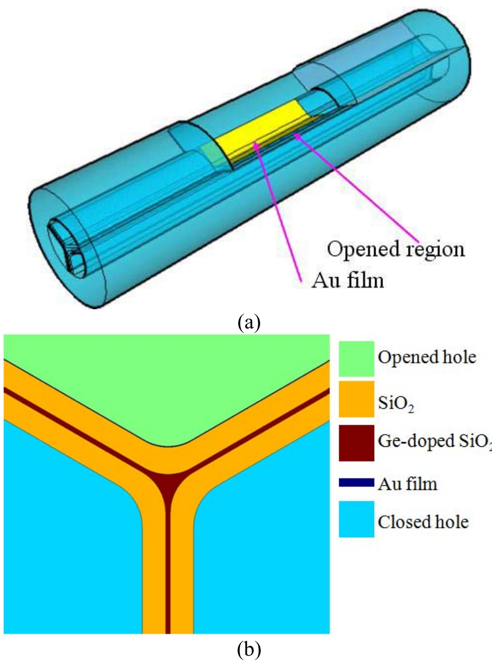

Fig. 1. Geometry of the proposed suspended core fiber SPR sensor. (a) Three dimensional sketch. (b) Cross sectional sketch.

fluid detection, especially when the target is in the dynamic environments. By special designing the fiber structure, a SPR sensor with a wide detecting range and a maximum sensitivity of 2.3e-5 RIU is achieved in simulation, which is in the same level with the sensitivity of side-closed suspended core fiber (1e-4RIU) [14]. The relationship of transmission loss spectrum characteristics, the thickness of Au film and the refractive index of target is also analyzed. Calculation results show that there is a close dependence among these parameters.

II. Geometry of the Proposed Fiber SPR Sensor

Geometry of the proposed side-opened suspended core fiber-based SPR sensor is given in Fig.1. To accelerate the fluid filling and access the fiber core, side hole can be opened on the silica-based suspended core fiber by use of FIB [22] or selective etching [23] or femtosecond laser techniques [2]. In this paper, the opening hole of the suspended core fiber is assumed to be filled with a liquid target of refractive index n. For the purpose of ensuring a strong mode confinement and a fundamental mode transmission the fiber struts are supposed to be a high index Ge-doped SiO_2 layer sandwiched between two layers consist of lower index pure SiO_2. The suspended core is formed of the three struts at their intersection region at the center position of fiber. To stimulate the surface plasmon resonance, the inner surface of the opening hole could be uniformly deposited with the Au-film by SAVAC sputter [20] or chemical deposition method [19]. Here, the lateral length of Au film deposited section and the overall transmission loss of the proposed fiber SPR sensor could be controlled flexibly according to the actual demand. For reducing the calculation time, only the upper surface of the suspended core and the adjacent strut region is supposed to be Au film deposited. As has been proved in reference [14], this assumption doesn't influence the accuracy of the calculation results. The radius of the Ge-doped core and the thickness of the struts of Ge-doped SiO_2 and SiO_2 are denoted as R, t_{Ge} and t_{SiO2} respectively.

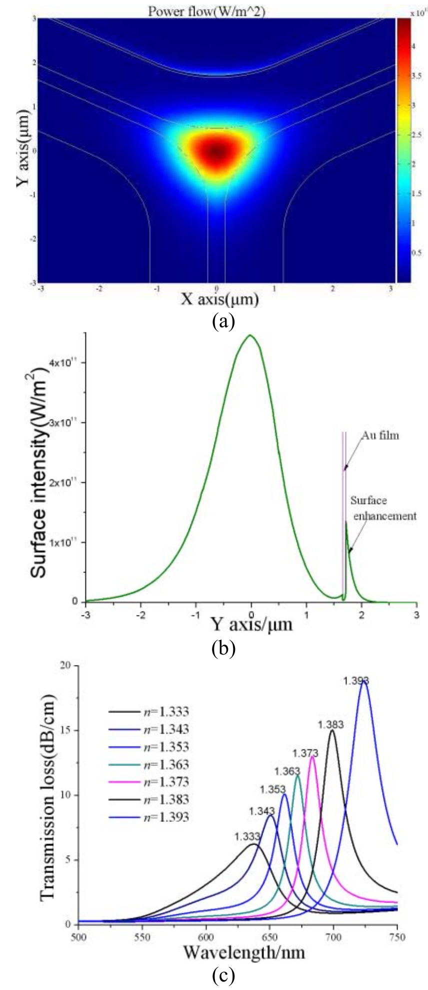

Fig. 2. Characteristics of the proposed suspended core fiber-based SPR sensor (R_{core} = 1200nm, t_{Au} = 50nm, $n = 1.333 \sim 1.393$, $\lambda = 500 \sim 750$nm, t_{Ge} = 300nm, t_{SiO2} = 1000nm). (a) Fundamental mode distributions, λ = 645nm. (b) X axis intensity distribution of the fundamental mode (y = 0, λ = 645nm). (c) Transmission loss spectrum characteristic of the fundamental mode.

The dielectric constant of the Au film here is got from the Drude model [23] and the refractive indices of SiO_2 and Ge-doped SiO_2 are got from the Sellmeier function [24]. The finite element method based software COMSOL multi-physics [14] and the perfectly matched layers boundary are utilized in simulation to find the complex effective mode index n_{eff} of the fiber modes over a wide wavelength range. $n_{eff} = \mathrm{Re}(n_{eff}) + i * \mathrm{Im}(n_{eff})$, $\mathrm{Re}(n_{eff}) = \beta\lambda/2\pi$ and $\mathrm{Im}(n_{eff}) = \alpha\lambda/2\pi$. Here α means the transmission loss constant, β represents the propagation constant [11] and λ is the operating wavelength. The real part of n_{eff} reflects the propagation constant and the imaginary part of n_{eff} is proportional to the transmission loss. As the SPR effect is mainly related with the TM polarization, only the fundamental mode characteristic of the TM polarization is analyzed in this paper. Fig. 2(a,b) shows the mode distribution characteristic of the side-opened suspended core fiber with a layer of Au film (R_{core} = 1200nm, t_{Au} = 50nm, n = 1.333, λ = 645nm,

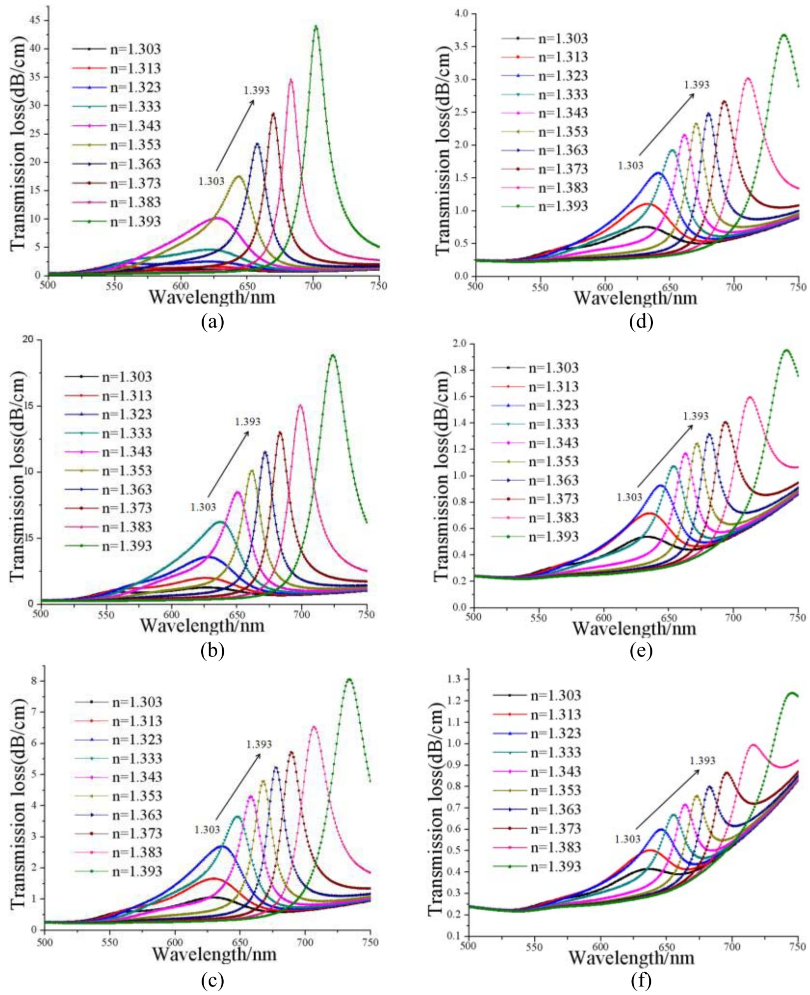

Fig. 3. The relation of Transmission loss and fluid index vs. different film thickness (R = 1200nm, t_{Ge} = 300nm, t_{SiO2} = 1000nm, $\lambda = 500 \sim 750$nm n = 1.303 ~ 1.393). (a) t_{Au} = 40nm. (b) t_{Au} = 50nm. (c) t_{Au} = 60nm. (d) t_{Au} = 70nm. (e) t_{Au} = 80nm. (f) t_{Au} = 90nm.

t_{Ge} = 300nm, t_{SiO2} = 100nm, $\Delta = (t_{Ge} - t_{SiO2})/t_{SiO2} = 1\%$). The inner surface of the side-opened hole is coated with Au film with thickness of t_{Au}. In fig.2, an enhanced and exponential damped field distribution appears at the outside surface of Au film, which is a characteristic of surface Plasmon excitation [14].

When the fiber fundamental mode energy is coupled into the Au film deposition region, the surface Plasmon mode could be excited. Tracking the transmission loss spectrum of the fundamental mode as a function of the operating wavelength, the transmission loss peak corresponding to the surface Plasmon resonance could be observed. Figure 2(c) shows the transmission spectrum characteristics, in which a sharp transmission loss peak appears within the operating waveband of 500nm~750nm. Monitoring the transmission loss spectrum characteristic, the refractive index of target could be calculated.

III. Analysis of the Fiber SPR Sensitivity

A. Transmission Loss Spectrum Characteristics

As the transmission loss spectrum characteristics of the fundamental mode is related with the thickness of Au film, fiber parameters and the refractive index of the target, those relations are analyzed firstly. Fig. 3(a-e) depicts the relation of transmission loss and the refractive index of target as a function of the wavelength and the thickness of Au film. It seems that a red-shift of peak wavelength and an increase of peak transmission loss appear with the increase of refractive index. While a red-shift of peak wavelength also occurs with the increase of the thickness of Au film. Therefore tracking the peak wavelength shift or the transmission loss at the fixed wavelength could distinguish the refractive index of the target. Depicting those relations could contribute to designing proper fiber SPR sensors for different demands.

Fig. 4(a) depicts the relation of the transmission loss and the fiber dimension. It seems that when the core radius R decreases from 1200nm to 400nm, the transmission loss increases. Fig. 4(b) shows that the fiber core size has little effect on the peak resonance wavelength when the filled fluid index is around 1.303~1.363. While the loss peak are separated when the filled fluid index becomes higher.

Fig. 5(a) and fig. 5(b) shows the relation of the transmission loss and the struts' thickness. It seems that the change of strut's thickness has little effect on the resonance wavelength characteristic. As a thicker strut could ensure the fundamental

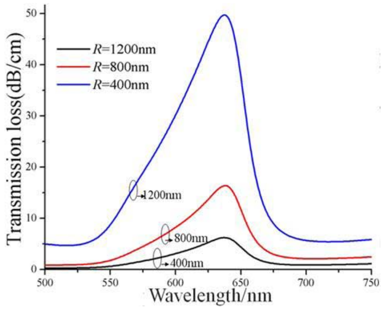

(a)

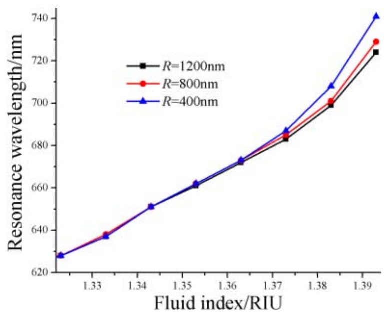

(b)

Fig. 4. Relation of transmission loss versus the fiber parameter R. (a) Transmission loss versus the core radius $R(t_{Ge} = 300\text{nm}\ t_{Au} = 50\text{nm})$. (b) Peak resonance wavelength versus core radius $R(t_{Ge} = 300\text{nm}\ t_{Au} = 50\text{nm})$.

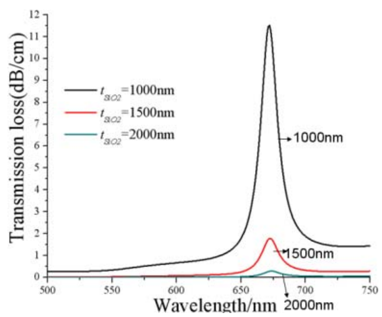

(a)

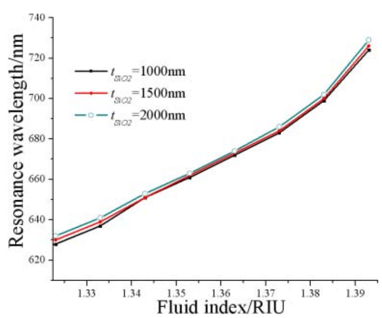

(b)

Fig. 5. Relation of transmission loss and the fiber parameter t_{SiO2}. (a) Transmission loss versus the thickness of the struts SiO_2 t_{SiO2} ($t_{Ge} = 300\text{nm}\ t_{Au} = 50\text{nm}$). (b) Relation of peak resonance wavelength and the thickness of the struts SiO_2 t_{SiO2} ($t_{Ge} = 300\text{nm}\ t_{Au} = 50\text{nm}$).

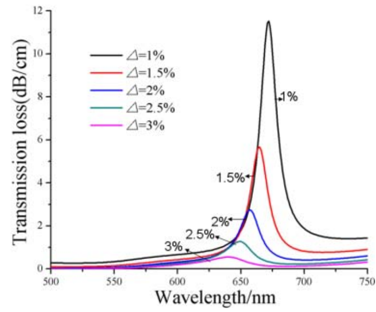

(a)

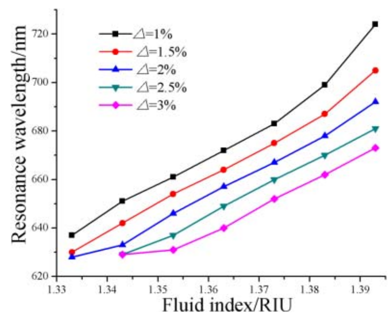

(b)

Fig. 6. Relation of transmission loss and the index contrast Δ. (a) Relation of transmission loss versus the index contrast $\Delta(t_{Ge} = 300\text{nm}\ t_{Au} = 50\text{nm})$. (b) Relation of peak resonance wavelength and the index contrast $\Delta(t_{Ge} = 300\text{nm}\ t_{Au} = 50\text{nm})$.

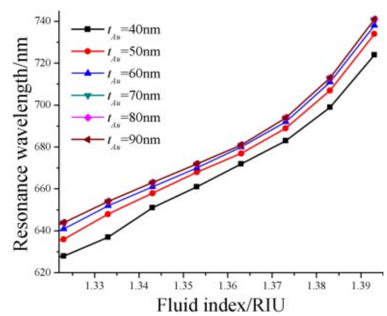

(a)

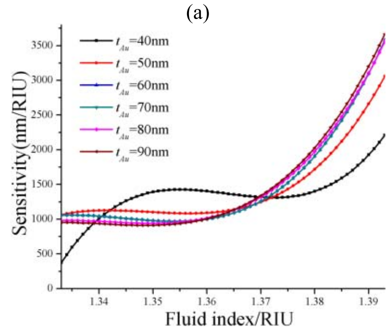

(b)

Fig. 7. Sensitivity characteristics of the SPR sensor based on monitoring the transmission loss spectrum peak shift. (a) Resonance wavelength shift versus film thickness and refractive index. (b) Sensitivity characteristic of the SPR sensor (fitted result).

mode transmission operation easily, a strut's thickness t_{SiO2} of 1000nm is used in the following discussions.

Fig. 6(a) reveals the relationship of transmission loss and index contrast Δ. It looks that the peak wavelength of the transmission loss has little effect on the index contrast Δ of Ge-doped SiO_2 and pure SiO_2. Our results are consistent with the results of ref [12]. Considering all these factors, 1200nm, 1000nm, 300nm and 1% are taken for R, t_{SiO2}, t_{Ge}, Δ respectively in the following simulation.

To analyze the specific sensing characteristics of the proposed fiber SPR sensor, two sensing mechanisms based on monitoring the transmission loss spectrum peak shift and

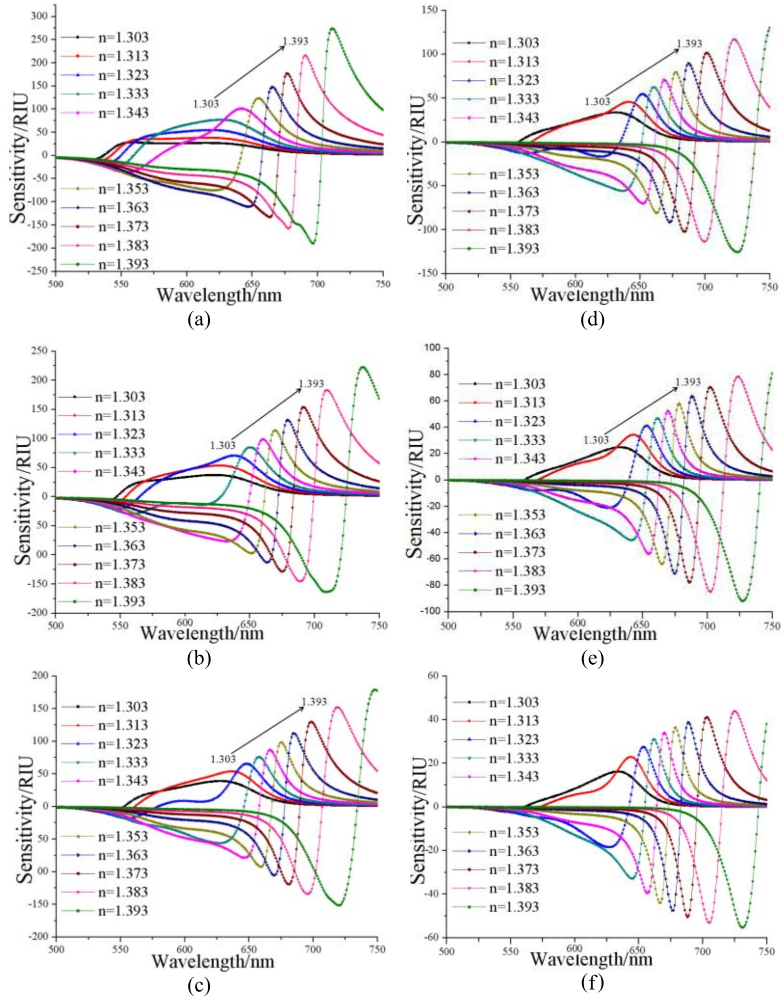

Fig. 8. Sensitivity based on monitoring the transmission power at a fixed wavelength (R = 1200nm, t_{Ge} = 300nm, t_{SiO2} =1000nm, Δ = 1%). (a) t_{Au} = 40nm. (b) t_{Au} = 50nm. (c) t_{Au} = 60nm. (d) t_{Au} = 70nm. (e) t_{Au} = 80nm. (f) t_{Au} = 90nm.

the transmission power change at the fixed wavelength are suggested and analyzed in the following sections.

B. Sensing Characteristics Based on Monitoring the Peak Shift of Transmission Loss Spectrum

In this section, a quantitative sensitivity characteristics based on monitoring the transmission loss spectrum peak shift is analyzed according to the sensitivity function [14]

$$S = \Delta\lambda_{peak}/\Delta\lambda n_a \tag{1}$$

$$\gamma = \Delta\lambda_{min}/S \tag{2}$$

Here, S represents the sensitivity, γ means the sensing resolution, Δn_a (equals to 0.01) denotes the change of refractive index, $\Delta\lambda_{min}$ represents the peak wavelength resolution, $\Delta\lambda_{peak}$ is the shift of resonance wavelength. Here the peak wavelength resolution $\Delta\lambda_{min}$ is assumed to be 0.1nm.

Fig. 7(a) shows the fitted results of the resonance wavelength shift characteristics. We notice that some experimental reports claim that the sensitivity is related with the thin film thickness [6]–[13]. But we find that there is no much difference in resonance wavelength shift versus refractive index curve for different thicknesses of film thickness in Fig. 7(a) as far as slopes are concerned. For quantitative analysis, Fig. 7(b) analyze the SPR sensitivity (fitted results) versus different fluid refractive indices. It means that the specific sensitivity characteristic has a little relation with the film thickness. A better sensitivity S of 3500 nm/RIU appears when the refractive index among 1.35~1.36 RIU. Here, the thickness of Au film is assumed to be 50nm. While the specific sensing resolution reported depends on the peak-wavelength resolution. Supposing the peak-wavelength resolution $\Delta\lambda_{min}$ is 0.1nm, the corresponding sensitivity resolution could reach up to 2.3e-5 RIU. It is in the same level with that of the hole-closed suspended core fiber-based SPR sensor [14]. The resolution parameter is referred to the reference [11]. The data of 0.1nm originates from the sensing resolution of fiber spectrometer. It should be noted that the relation of sensitivity and film thickness is not obvious in current simulation condition. Further study on the relationship would be conducted by introducing more possible impact factors in modeling is in progress.

C. Sensing Characteristics Based on Monitoring the Transmission Power at the Fixed Wavelength

Here, another sensing mechanism based on monitoring the transmission power at the fixed wavelength is analyzed and compared. For this sensing mechanism, two sensitivity parameters (S and γ) [15] are introduced for analysis.

$$S = (\Delta\alpha/\Delta n_a)/\alpha_{na} \tag{3}$$

$$\gamma = \Delta_p/S \tag{4}$$

Here, S denotes the sensitivity. α_{na} represents the transmission loss, the refractive index of target is set as n_a, γ means the sensing resolution. 1% change (Δ_p) of transmission power is assumed to be reliably measured. The difference of n_a equals to 0.001.

Fig. 8(a-f) shows the sensitivity characteristic of fiber SPR sensors with different Au film based on the second measurement method. It seems the specific sensitivity resolution is related with the specific operating wavelength and the thickness of Au film. With the increase of Au film thickness, the refractive index range of better sensitivity moves to a higher index region. Besides, the sensitivity resolution reaches its best when the operating wavelength is close to the resonance wavelength. It also appears the sensing resolution is straightly related with the refractive index of the target. With the increase of fluid index, the maximal sensitivity also increases too. The maximal sensitivity of 161/RIU appears when t_{Au} equals to 40nm and n equals to 1.363. The corresponding sensitivity resolution could reach up to 3.65e-5 RIU (supposing Δ_p equals to 1%).

By comparing the aforementioned two sensing mechanisms, we find that the maximal resolutions of both methods are in the same order of magnitude. However it seems the transmission loss spectrum peak shift sensing mechanism owns the characteristics of wide sensing region. In addition, the detected refractive index range of maximal resolution based on the transmission loss spectrum peak shift sensing mechanism near 1.33 RIU (the index of water), which seems more useful for fluid detection. Furthermore, transmission loss spectrum peak shift sensing mechanism is also irrespective to the transmission power fluctuation. So, the SPR sensing mechanism based on transmission loss spectrum may exhibit more advantages in practical applications.

IV. Conclusion

Finally, a new side-opened suspended core fiber surface Plasmon resonance sensor with a single-hole Au-deposited film configuration is proposed and analyzed. The presented design has the following advantages: First, the removed side cladding facilitates the fabrication of the SPR sensor structure and speeds up the response. Second, the metallic film contributes to enhance the resonance status for SPR sensing. By suitably designing, a wide detected range with high optical sensitivity of 2.3e-5 RIU is achieved in simulation. The sensitivity value is close to that of the other reported counterpart without side opening.

References

[1] J. Homola, "Present and future of surface plasmon resonance biosensors," *Anal. Bioanal. Chem.*, vol. 377, no. 3, pp. 528–539, Oct. 2003.

[2] A. J. C. Tubb, F. P. Payne, R. B. Millington, and C. R. Lowe, "Single-mode optical fibre surface plasma wave chemical sensor," *Sens. Actuators B, Chem.*, vol. 41, nos. 1–3, pp. 71–79, Jun. 1997.

[3] A. Trouillet, C. Ronot-Trioli, C. Veillas, and H. Gagnaire, "Chemical sensing by surface plasmon resonance in a multimode optical fibre," *Pure Appl. Opt., J. Eur. Opt. Soc. A*, vol. 5, no. 2, pp. 227–237, 1996.

[4] A. Hassani and M. Skorobogatiy, "Design of the microstructured optical fiber-based surface plasmon resonance sensors with enhanced microfluidics," *Opt. Exp.*, vol. 14, no. 24, pp. 11616–11621, Nov. 2006.

[5] Y. Wang, X. Tan, W. Jin, D. Ying, Y. L. Hoo, and S. Liu, "Temperature-controlled transformation in fiber types of fluid-filled photonic crystal fibers and applications," *Opt. Lett.*, vol. 35, no. 1, pp. 88–90, 2010.

[6] Y.-P. Wang, J.-P. Chen, and Y.-J. Rao, "Torsion characteristics of long-period fiber gratings induced by high-frequency CO_2 laser pulses," *J. Opt. Soc. Amer. B*, vol. 22, no. 6, pp. 1167–1172, 2005.

[7] C. Wang *et al.*, "Highly birefringent suspended-core photonic microcells for refractive-index sensing," *Appl. Phys. Lett.*, vol. 105, no. 6, pp. 061105-1–061105-4, Aug. 2014.

[8] A. Hassani and M. Skorobogatiy, "Design criteria for microstructured-optical-fiber-based surface-plasmon-resonance sensors," *J. Opt. Soc. Amer. B*, vol. 24, no. 6, pp. 1423–1429, 2007.

[9] B. Gauvreau, A. Hassani, M. F. Fehri, A. Kabashin, and M. Skorobogatiy, "Photonic bandgap fiber-based surface plasmon resonance sensors," *Opt. Exp.*, vol. 15, no. 18, pp. 11413–11426, 2007.

[10] M. Hautakorpi, M. Mattinen, and H. Ludvigsen, "Surface-plasmon-resonance sensor based on three-hole microstructured optical fiber," *Opt. Exp.*, vol. 16, no. 12, pp. 8427–8432, 2008.

[11] C. Guan, Y. Wang, and L. Yuan, "Multi-hole optical fiber surface plasmon resonance sensor," *J. Phys., Conf. Ser.*, vol. 276, no. 1, pp. 012057-1–012057-6, 2011.

[12] C. Perrotton, N. Javahiraly, M. Slaman, B. Dam, and P. Meyrueis, "Fiber optic surface plasmon resonance sensor based on wavelength modulation for hydrogen sensing," *Opt. Exp.*, vol. 19, no. S6, pp. A1175–A1183, Nov. 2011.

[13] C. Gu *et al.*, "Recent advance in fiber SERS sensors," *Proc. SPIE Photon. Fiber Crystal Devices, Adv. Mater. Innov. Device Appl. II*, vol. 7056, p. 70560H, Aug. 2008.

[14] S. Smolka, M. Barth, and O. Benson, "Selectively coated photonic crystal fiber for highly sensitive fluorescence detection," *Appl. Phys. Lett.*, vol. 90, no. 11, 2007, Art. ID 111101.

[15] H.-Y. Lin, C.-H. Huang, G.-L. Cheng, N.-K. Chen, and H.-C. Chui, "Tapered optical fiber sensor based on localized surface plasmon resonance," *Opt. Exp.*, vol. 20, no. 19, pp. 21693–21701, Sep. 2012.

[16] A. Wang, A. Docherty, B. T. Kuhlmey, F. M. Cox, and M. C. J. Large, "Side-hole fiber sensor based on surface plasmon resonance," *Opt. Lett.*, vol. 34, no. 24, pp. 3890–3892, 2009.

[17] Y.-H. Luo *et al.*, "Spectra modulated surface plasmon resonance sensor based on side polished multi-mode optical fiber," *Spectrosc. Spectral Anal.*, vol. 34, no. 3, pp. 577–581, 2014.

[18] H.-Y. Lin, W.-H. Tsai, Y.-C. Tsao, and B.-C. Sheu, "Side-polished multimode fiber biosensor based on surface plasmon resonance with halogen light," *Appl. Opt.*, vol. 46, no. 5, pp. 800–806, Feb. 2007.

[19] G. Wang, J. Liu, Y. Yang, Z. Zheng, J. Xiao, and R. Li, "Gas Raman sensing with multi-opened-up suspended core fiber," *Appl. Opt.*, vol. 50, no. 31, pp. 6026–6032, May 2011.

[20] G. Wang *et al.*, "Fluidic sensor based on the side-opened and suspended dual-core fiber," *Appl. Opt.*, vol. 51, no. 15, pp. 3096–3103, May 2012.

[21] C. M. B. Cordeiro *et al.*, "Towards practical liquid and gas sensing with photonic crystal fibres: Side access to the fibre microstructure and single-mode liquid-core fibre," *Meas. Sci. Technol.*, vol. 18, no. 10, pp. 3075–3081, Feb. 2007.

[22] W. Zhu, T. Shi, Z. Tang, B. Gong, G. Liao, and J. Tully, "Dynamic selective etching: A facile route to parabolic optical fiber nano-probe," *Opt. Exp.*, vol. 21, no. 6, pp. 6919–6927, Mar. 2013.

[23] P. B. Johnson and R. W. Christy, "Optical constants of the noble metals," *Phys. Rev. B*, vol. 6, no. 12, pp. 4370–4379, 1972.

[24] M. J. Weber, *Hand Book of Optical Materials*. Boca Raton, FL, USA: CRC Press, 2003.

Guanjun Wang received the B.S. degree in electronic science and technology and the M.S. degree in physical electronics from Zhengzhou University, Zhengzhou, China, in 2005 and 2008, respectively, and the Ph.D. degree in optical engineering from Beihang University, Beijing, China, in 2012.

He was with the North University of China, Taiyuan, China, as a Lecturer, after the graduation.

He is currently a Post-Doctoral Researcher with the Institute of Optoelectronic Devices and Systems of Ministry of Education and Guangdong Province, College of Optoelectronic Engineering, Shenzhen University, Shenzhen, China.

His research interests include fiber biochemical sensors and fiber grating.

Chao Wang, photograph and biography not available at the time of publication.

Shen Liu, photograph and biography not available at the time of publication.

Jing Zhao, photograph and biography not available at the time of publication.

Changrui Liao, photograph and biography not available at the time of publication.

Xizhen Xu, photograph and biography not available at the time of publication.

Haijian Liang, photograph and biography not available at the time of publication.

Guolu Yin, photograph and biography not available at the time of publication.

Yiping Wang (M'04–SM'06) received the B.S. degree in precision instrument engineering from the Xi'an Institute of Technology, Xi'an, China, in 1995, and the M.S. degree in precision instrument and mechanism and the Ph.D. degree in optical engineering from Chongqing University, Chongqing, China, in 2000 and 2003, respectively, where he received the prestigious National Excellent Doctoral Dissertations Award in China.

He joined the Department of Electronics Engineering, Shanghai Jiao Tong University, Shanghai, China, as a Post-Doctoral Research Fellow and an Associate Professor, in 2003. In 2005, he joined the Department of Electrical Engineering, Hong Kong Polytechnic University, Hong Kong, as a Post-Doctoral Research Fellow and Research Fellow. In 2007, he joined the Institute of Photonic Technology, Jena, Germany, as a Humboldt Research Fellow, and the Optoelectronics Research Centre, University of Southampton, Southampton, U.K., as a Marie Curie Fellow, in 2009. Since 2012, he has been with Shenzhen University, Shenzhen, China, as a Distinguished Professor and Pearl River Scholar. His current research interests focus on optical fiber sensors, in-fiber gratings, photonic crystal fibers, and fluid-filling technologies. He has authored or co-authored one book, nine patent applications, and over 150 journal and conference papers with a SCI citation of more than 1200 times.

Dr. Wang is currently a Senior Member of the Optical Society of America, and the Chinese Optical Society.